Contribution from the Department of Chemistry,
University of South Carolina, Columbia, South Carolina 29208

Spectra and Structure of Organophosphorus Molecules. 39.[†] Microwave, Raman, and Infrared Spectra of Trimethylphosphine Sulfide and Three Deuteriated Species

J. R. Durig* and K. K. Chatterjee

Microwave spectra from 26.5 to 39.0 GHz of $(CH_3)_3PS$, $(CH_3)_2(CD_3)PS$, $(CH_3)(CD_3)_2PS$, $(CD_3)_3PS$, and $(CH_3)_3P^{34}S$ have been measured at ambient temperature, and the observed transitions have been assigned for the ground vibrational states for each molecule. From a diagnostic least-squares adjustment to fit nine independent rotational constants, the following r^0 structural parameters were obtained: $r(P{=}S) = 1.936 \pm 0.003$ Å, $r(P{-}C) = 1.814 \pm 0.001$ Å, $r(C{-}H) = 1.094 \pm 0.003$ Å, $\angle CPS = 114.36 \pm 0.09°$, $\angle HCH = 109.52 \pm 0.04°$, and methyl tilt angle of $3.7 \pm 1.3°$. The bond length for the P=S bond lies close to the value expected for a double bond, and it is in agreement with the previously reported value for this bond from an electron diffraction study. The low-temperature mid-infrared spectra (3200–500 cm^{-1}) and the Raman spectra (3200–50 cm^{-1}) at ambient temperature have also been recorded for the solid states of all five isotopic species. The far-infrared spectra of the d_0 and d_9 species have also been measured as Nujol mulls. Assignments of the fundamental vibrations have been made by assuming an effective C_{3v} symmetry for $(CH_3)_3PS$ and $(CD_3)_3PS$ and C_s symmetry for $(CH_3)_2(CD_3)PS$ and $(CH_3)(CD_3)_2PS$. The proposed assignment of the normal modes is supported by a normal-coordinate calculation utilizing a simple valence force field to calculate the fundamental frequencies and the potential energy distribution. These results are compared to corresponding quantities for some similar molecules.

Introduction

Trimethylphosphine, as well as trimethylarsine, forms stable adducts with oxygen and sulfur atoms and these compounds are of considerable interest because of the possibility of multiple bonding between the donor and acceptor atoms. At temperatures ranging from 150 to 175 °C gas-phase electron diffraction studies of the oxides and sulfides of $(CH_3)_3P$ and $(CH_3)_3As$ by Wilkins et al.[1] have shown that the phosphorus–sulfur and arsenic–sulfur bond lengths lie close to values expected for classical double bonds but the phosphorus–oxygen and arsenic–oxygen distances are especially short, corresponding to even higher bond orders. Both $(CH_3)_3PO$ and $(CH_3)_3PS$ are solids at ambient temperature, but both have appreciable vapor pressure, which permitted a study of the microwave spectra of these compounds. While investigations of the entire series of these adducts are in progress, in the present paper the structural information that has been obtained for $(CH_3)_3PS$ and its deuteriated species is described. Additionally, the Raman and low-temperature infrared spectra of these compounds are also reported and discussed in detail.

Experimental Section

The sample of $(CH_3)_3PS$, obtained from Alfa Inorganics, was purified by sublimation under vacuum. For the preparation of the deuteriated species the required deuteriated phosphines, $(CD_3)_3P$, $(CD_3)_2(CH_3)P$, and $(CD_3)(CH_3)_2P$, were first synthesized by treating PCl_3, CH_3PCl_2, and $(CH_3)_2PCl$, respectively, with CD_3MgI and the products isolated as previously described.[2] The following method was used for obtaining the sulfur adducts. About 150–200 mg of freshly sublimed sulfur was suspended in 5 mL of dry diethyl ether in a 25-mL pyrex glass reaction tube, which was then attached to the vacuum line. The suspension was frozen by boiling liquid N_2 and outgassed, and approximately 2.5 mL of the deuteriated phosphine was condensed into the reaction tube, which was slowly warmed to room temperature with constant stirring. Stirring was continued (at least for 6 h) with intermittent freezing and warming of the mixture to room temperature until the pale yellow color due to unreacted sulfur disappeared. After removal of the ether under vacuum, the residual white solid products were first sublimed under vacuum and further purified by recrystallization from solution in carbon disulfide. The sample of $(CH_3)_3P^{34}S$ was also prepared by the aforesaid method using $(CH_3)_3P$ (Alfa) and ^{34}S obtained from Icon Services, Inc.

The microwave spectra of the sulfur adducts were recorded in the region 26.5–39 GHz by using a Hewlett-Packard Model 8460A MRR spectrometer with a Stark modulation frequency of 33.3 kHz. The spectra were measured with the waveguide at ambient temperature, the pressure of the sample being maintained around 15 μmHg. The measured frequencies are estimated to be reliable to ±0.05 MHz.

A Cary Model 82 Raman spectrophotometer, calibrated with atomic Hg or Ne emission lines, was used to record the Raman spectra of the

Table I. Observed Ground-State Transitions and Rotational Constants (MHz) and Centrifugal Distortion Constants (kHz) for $(CH_3)_3PS$ and $(CD_3)_3PS^a$

molecule	transition	ν_{obs}	B_0	D_J
$(CH_3)_3P^{32}S$	6 ← 5	28 299.35	2358.30 ± 0.01	0.30 ± 0.01
	7 ← 6	33 015.80		
	8 ← 7	37 732.20		
$(CD_3)_3P^{32}S$	7 ← 6	28 322.60	2023.07 ± 0.01	0.28 ± 0.01
	8 ← 7	32 368.56		
	9 ← 8	36 414.45		
$(CH_3)_3P^{34}S$	6 ← 5	27 582.72	2298.58 ± 0.01	0.27 ± 0.01
	7 ← 6	32 179.74		
	8 ← 7	36 776.72		

^{a} Reported errors are standard errors.

solid samples from 3200 to 50 cm^{-1} (Figures 1 and 2). A Spectra-Physics Model 171 argon ion laser, tuned to the 5145-Å line, was employed as the excitation source. Samples were introduced into Pyrex capillary tubes of 1.5-mm diameter, which were then sealed under vacuum. Spectra were obtained at room temperature with the laser power on the samples not exceeding 0.25 W to prevent thermal effects. The spectral band width was held fixed at 3 cm^{-1} in all measurements. The frequencies of the sharp, resolvable lines are estimated to be accurate to within ±2 cm^{-1}.

The low-temperature mid-infrared spectra of the solids (Figures 3 and 4) were obtained in the range 3200–500 cm^{-1} by using a Digilab Model FTS-14C Fourier transform interferometer equipped with a high-intensity Globar source, a Ge/KBr beam splitter, and a TGS detector. The spectrophotometer housing was purged with dry N_2. Samples were slowly deposited, by sublimation under vacuum, onto a CsI substrate that was mounted on a brass block in thermal contact with a reservoir of boiling liquid N_2. Spectra in the far-infrared region (400–50 cm^{-1}) for $(CH_3)_3PS$ and $(CD_3)_3PS$ (Figure 5) were obtained as Nujol mulls by using a Digilab Model FTS-15B interferometer equipped with a Mylar beam splitter of 6.25 μm thickness and a high-pressure mercury lamp. A resolution of 2 cm^{-1} and 200 coadded scans for both the samples and backgrounds were used to obtain the spectral data with the Fourier transform interferometers.

Microwave Spectra

The microwave spectra of $(CH_3)_3PS$, $(CD_3)_3PS$, and $(CH_3)_3P^{34}S$ are typically those of a prolate symmetric top. Three transitions were measured for each species, and they are listed in Table I, with the derived values of the rotational constants, B_0, and the centrifugal distortion constants, D_J. Each ground-state transition is associated with a large number of strong satellites arising from excited vibrational states, the essential features of

(1) Wilkins, C. J.; Hagen, K.; Hedberg, L.; Shen, Q.; Hedberg, K. *J. Am. Chem. Soc.* **1975**, *97*, 6352.
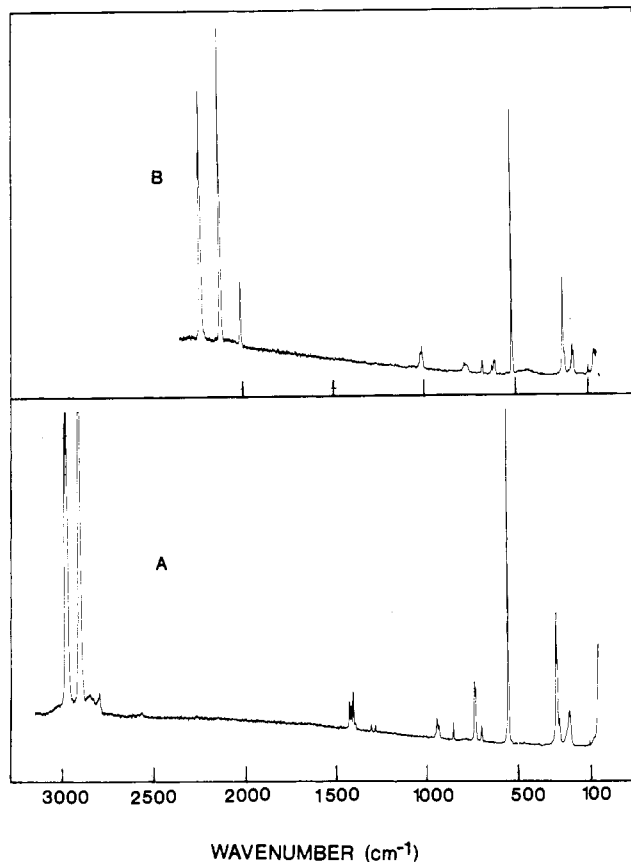(2) Mann, F. G.; Wells, A. F. *J. Chem. Soc.* **1938**, 708.

WAVENUMBER (cm⁻¹)

Figure 1. Raman spectra of (A) solid $(CH_3)_3PS$ and (B) solid $(CD_3)_3PS$ recorded at ambient temperature.

WAVENUMBER (cm⁻¹)
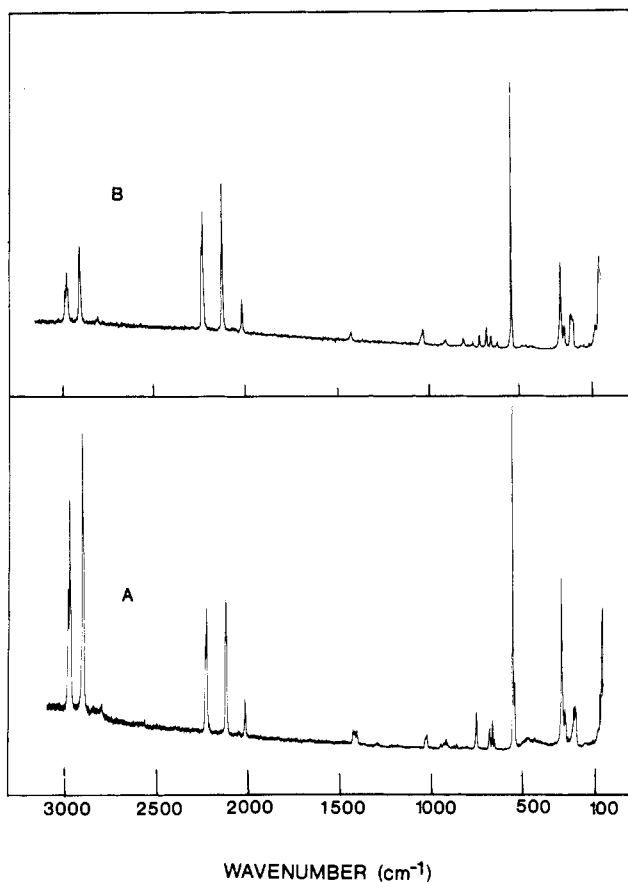
Figure 2. Raman spectra of (A) solid $(CH_3)_2CD_3PS$ and (B) solid $CH_3(CD_3)_2PS$ recorded at ambient temperature.

the observed patterns being similar for each transition. No attempt, however, has been made to assign transitions arising from
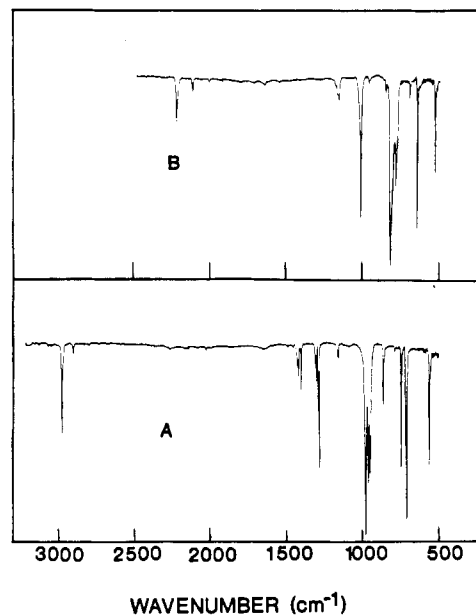

WAVENUMBER (cm⁻¹)

Figure 3. Mid-infrared spectra of (A) $(CH_3)_3PS$ and (B) $(CD_3)_3PS$ recorded at 77 K.

WAVENUMBER (cm⁻¹)
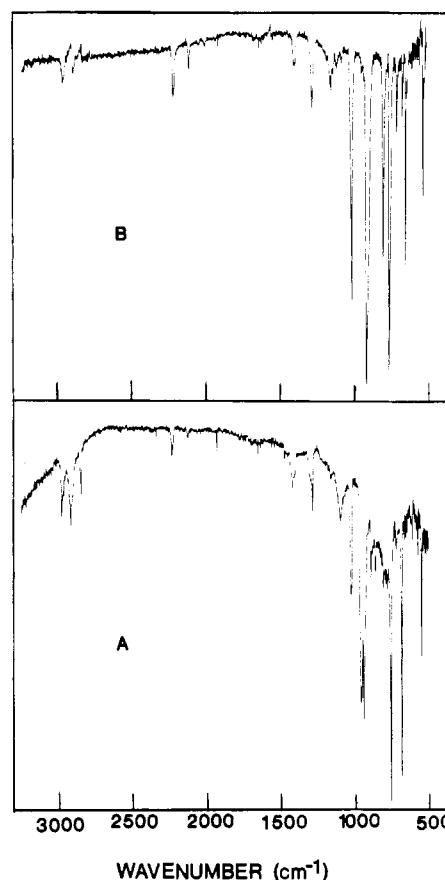
Figure 4. Mid-infrared spectra of (A) $(CH_3)_2CD_3PS$ and (B) $CH_3(C-D_3)_2PS$ recorded at 77 K.

the vibrational satellites resulting from the methyl torsional modes and the low-frequency skeletal bending motions.

Due to the partial substitution of the methyl groups by CD_3 groups, the 3-fold symmetry axis is not retained in $(CH_3)_2(CD_3)PS$ and $(CH_3)(CD_3)_2PS$, and the effective symmetry for these molecules is reduced to C_s. Only the strong A-type transitions were measured, although less intense B- and C-type transitions are also expected to occur in the d_3 and d_6 species, respectively. The measured transitions are listed in Table II, and for both cases the assignments for the transitions were confirmed by measuring the dependence of the line intensities on the applied Stark voltages

WAVENUMBER (cm⁻¹)

Figure 5. Far-infrared spectra of (A) $(CH_3)_3PS$ and (B) $(CD_3)_3PS$ in Nujol mulls.

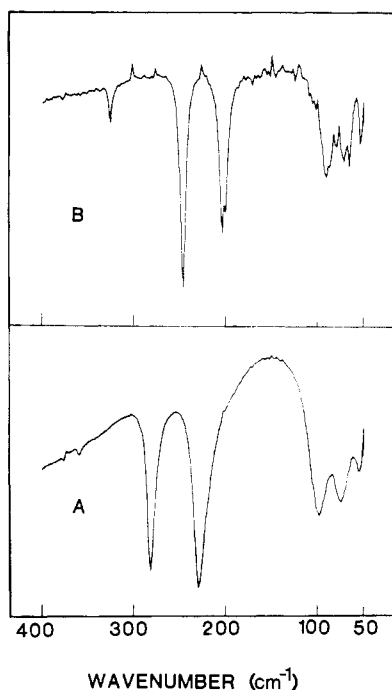**Table II.** Rotational Transitions (MHz), Rotational Constants (MHz), and Centrifugal Distortion Constants (kHz) in the Ground Vibrational States of $(CH_3)_2CD_3PS$ and $CH_3(CD_3)_2PS$[a]

	$(CH_3)_2CD_3PS$		$CH_3(CD_3)_2PS$	
transition	ν(obs)	$\Delta\nu$ (obs − calc)	ν(obs)	$\Delta\nu$ (obs − calc)
$7_{17} \leftarrow 6_{16}$	30856.90	0.01	29277.55	−0.01
$7_{07} \leftarrow 6_{06}$	30969.85	0.06	29365.46	−0.03
$7_{26} \leftarrow 6_{25}$	31211.90	0.00	29652.48	−0.01
$7_{16} \leftarrow 6_{15}$	31496.02	0.01	29933.30	0.02
$7_{25} \leftarrow 6_{24}$	31502.40	0.09	30001.70	0.03
$8_{18} \leftarrow 7_{17}$	35245.02	−0.07	33436.85	0.04
$8_{08} \leftarrow 7_{07}$	35333.27	−0.01	33499.68	−0.01
$8_{27} \leftarrow 7_{26}$	35650.05	0.04	33861.88	0.00
$8_{17} \leftarrow 7_{16}$	35949.65	0.03	34146.76	0.01
$8_{26} \leftarrow 7_{25}$	36040.74	−0.08	34318.15	−0.03

$A = 3310.00 \pm 0.28$ $A = 3034.76 \pm 0.10$

$B = 2280.94 \pm 0.01$ $B = 2173.19 \pm 0.01$

$C = 2185.00 \pm 0.01$ $C = 2072.14 \pm 0.01$

$D_J = 0.21 \pm 0.06$ $D_J = 0.29 \pm 0.04$

$\kappa = -0.8294$ $\kappa = -0.7900$

[a] Reported errors are standard errors.

and the rigid-rotor fit. No torsional splittings were observed for the ground-state lines. The effective rotational constants for the asymmetric tops are listed in Table II. Because the measured transitions are relatively insensitive to the A rotational constant, the uncertainties of the A rotational constants are relatively large compared to those for the B and C rotational constants.

Structure

In order to determine the r_0 structure, the structural parameters that best fit the nine effective rotational constants of the five isotopic species (Tables I and II) were calculated by using the method of diagnostic least-squares described by Groner et al.[3] The structural parameters, initially chosen for this purpose, and the adjusted parameters for two probable structures for $(CH_3)_3P$=S are listed in Table III. In both cases the methyl groups are symmetrical, but contrary to the case of structure I, in structure II the symmetry axis of the CH_3 group is not collinear with the

P–C bond axis and each CH_3 groups has an upward tilt of approximately 3.7° toward the phosphorus–sulfur bond. Moreover, unlike those in structure I, all the PCH angles in structure II are not equal ($\angle PCH^s = 113.17 \pm 1.25°$; $\angle PCH^a = 107.52 \pm 0.69°$). However, the values of the P–S and P–C bond distances and the CPS bond angle are approximately the same in both structures I and II and these are in excellent agreement with the corresponding parameters reported earlier from an electron diffraction study of $(CH_3)_3PS$ by Wilkins et al.,[1] as shown in Table III. On the other hand, differences are observed in the values of the C–H bond lengths that are obtained by the two independent methods of structure determinations.

Vibrational Spectra and Assignments

Previous vibrational assignments of the fundamental modes of $(CH_3)_3PS$ and $(CD_3)_3PS$, by Rojhantalab et al.,[4] were based on the Raman spectra of single crystals and those of sublimed films of these compounds at 190 and 14 K, respectively. Although a factor group of C_{2h} where the two molecules of the primitive cell occupy C_s sites is suggested by the X-ray diffraction study[5] of solid $(CH_3)_3PS$, most of the spectra of the sublimed films of both isotpic species could be interpreted by using only C_{3v} molecular symmetry. However, the infrared spectra of both $(CH_3)_3PS$ and $(CD_3)_3PS$, which we measured, reveal certain features that are absent in the Raman effect. These and other considerations have prompted us to reassign some of the fundamental modes of these compounds. The infrared frequencies of $(CH_3)_3PS$, $(CD_3)_3PS$, $(CH_3)_2(CD_3)PS$, and $(CH_3)(CD_3)_2PS$ and the frequencies of the corresponding Raman lines, measured at room temperature, have listed in Tables IV–VII, respectively.

The descriptions for the fundamental modes with their potential energy distributions, as presented in the tables of vibrational frequencies, were derived from the normal-coordinate calculations. A force field was first constructed to fit the observed frequencies for the d_0 and d_9 species and then used to predict the frequencies of the d_3 and d_6 species. This procedure led to satisfactory assignments of the observed frequencies in all four cases. The details of the normal-coordinate calculations will be given in a later section. We shall briefly review the changes that we are proposing for the assignments for some of the normal modes for $(CH_3)_3PS$ and $(CD_3)_3PS$ (Tables IV and V) compared to those given earlier.[4]

In the regions of the CH_3 stretching and bending motions, the assignments of the fundamental frequencies for $(CH_3)_3PS$ and $(CD_3)_3PS$ are generally in accord with the earlier work.[4] However, the strong infrared band observed at 981 cm⁻¹ in the spectrum of $(CH_3)_3PS$ and the two bands at 968 and 822 cm⁻¹ in the infrared spectrum of $(CD_3)_3PS$ show no counterparts in the Raman spectra. We thus assign the 981-cm⁻¹ band in the "light" compound to a CH_3 rock, $\nu_{19}(E)$, and the band at 968 cm⁻¹ in the d_9 species to a symmetric CD_3 deformational motion, $\nu_{18}(E)$.

The bands observed at 647 cm⁻¹, $\nu_5(A_1)$, and 630 cm⁻¹, $\nu_{20}(E)$, in the Raman spectrum of $(CD_3)_3PS$, which appear at approximately the same frequencies in the infrared spectrum, were previously[4] attributed to the PC_3 symmetric and PC_3 antisymmetric stretching modes, respectively. From the potential energy distribution for the modes of $(CD_3)_3PS$, the PC_3 antisymmetric and symmetric stretches are more appropriately assigned to the strong infrared bands observed at 822 cm⁻¹, $\nu_{21}(E)$ and 648 cm⁻¹, $\nu_5(A_1)$, respectively. Obviously, the 630-cm⁻¹ band, $\nu_{20}(E)$, which arises mainly from a CD_3 rocking motion, is mixed with the PC_3 antisymmetric stretch. Actually, neither of the two PC_3 stretching modes may be characterized by a single frequency in the spectrum of $(CD_3)_3PS$, as both are extensively coupled with the CD_3 rocking motions. The strong Raman band at 536 cm⁻¹ (infrared band at 531 cm⁻¹) in the spectrum of $(CD_3)_3PS$, which was previously assigned to the P=S stretching motion, is also due to a composite motion in which the P=S stretch is strongly coupled with the PC_3 symmetric stretch. The earlier investigators[4] would have certainly

(3) Groner, P.; Church, J. S.; Li, Y. S.; Durig, J. R. *J. Chem. Phys.* **1985**, *53*, 3894.

(4) Rojhantalab, H.; Nibler, J. W.; Wilkins, C. J. *Spectrochim. Acta* **1976**, *32A*, 519.

(5) Eller, P. G.; Corfield, P. W. R. *J. Chem. Soc.* **1969**, *19A*, 2927.

Table III. Diagnostic Least-Squares Adjustment of the Structural Parameters of $(CH_3)_3PS$ and Calculated Rotational Constants (MHz)

param[a]	initial value	estd uncertainty	adjusted value for I[b]	adjusted value for II[b]	electron diffraction value[1,c]
$r(P=S)$, Å	1.940	±0.020	1.940 ± 0.004	1.936 ± 0.003	1.940 ± 0.002
$r(P-C)$, Å	1.818	±0.020	1.814 ± 0.002	1.814 ± 0.001	1.818 ± 0.002
$r(CH)$, Å	1.093	±0.020	1.087 ± 0.002	1.094 ± 0.003	1.106 ± 0.005
∠CPS, deg	114.10	±2.00	114.23 ± 0.12	114.36 ± 0.09	114.1 ± 0.2
∠PCH^s, deg	109.54[d]	±2.00	109.53 ± 0.04	113.17 ± 1.25[e]	108.6 ± 0.8
∠PCH^a, deg	109.54[d]	±2.00	109.53 ± 0.04	107.52 ± 0.69[e]	108.6 ± 0.8
∠H^{s}CH^a	109.44[f]	±2.00	109.41 ± 0.04[e]	109.52 ± 0.04	
∠H^{a}CH^a	109.44[f]	±2.00	109.41 ± 0.04[e]	109.52 ± 0.04	
tilt angle, deg	2.5	±2.00		3.74 ± 1.28	

			structure I		structure II	
molecule	rotational const	obs[g]	calc	Δ (obs − calc)	calc	Δ (obs − calc)
$(CH_3)_3PS$	B	2358.60	2358.37	−0.07	2358.32	−0.02
$(CH_3)_2CD_3PS$	A	3310.00	3309.95	0.05	3310.37	−0.37
	B	2280.94	2280.84	0.10	2280.88	0.06
	C	2185.00	2185.01	−0.01	2185.04	−0.04
$CH_3(CD_3)_2PS$	A	3034.76	3034.75	0.01	3034.33	0.43
	B	2173.19	2173.19	−0.00	2173.22	−0.03
	C	2072.14	2072.06	0.08	2072.09	0.05
$(CD_3)_3PS$	B	2023.07	2023.12	−0.05	2023.08	−0.01
$(CH_3)_3P^{34}S$	B	2298.58	2298.55	0.03	2298.57	0.01

[a] The angles indicated by a and s are antisymmetric and symmetric, respectively, with respect to the plane through the methyl groups. [b] Errors given are standard errors. [c] These parameters are for the model that gave a torsional angle (42.7 ± 7.3°) for each of the methyl groups. [d] Initial value for structure I only. [e] Calculated from other parameters for comparison. [f] Initial value for structure II only. [g] The following errors were assumed for weighting purposes: 1.0 MHz for A; 0.1 MHz for B and C.

Table IV. Assignment of Fundamental Vibrations[a] for Trimethylphosphine Sulfide

IR ν, cm^{-1}	Raman Δν, cm^{-1}	calc ν, cm^{-1}	assgnt and pot. energy distribn
	2981 s	2982	ν_{13}(E), CH$_3$ antisym str (100%)
2976	2973 vs	2981	ν_1(A$_1$), CH$_3$ antisym str (100%)
	2973 vs	2979	ν_{14}(E), CH$_3$ antisym str (100%)
2903 w	2903 s	2895	ν_2(A$_1$), CH$_3$ sym str (100%)
	2897 sh	2895	ν_{15}(E), CH$_3$ sym str (100%)
1427 w	1431 w	1427	ν_{16}(E), CH$_3$ antisym def (94%)
1423 w	1422 w	1425	ν_3(A$_1$), CH$_3$ antisym def (95%), CH$_3$ rock (5%)
	1422	1420	ν_{17}(E), CH$_3$ antisym def (94%)
1310, 1303 } w	1131 w	1314	ν_4(A$_1$), CH$_3$ sym def (95%)
1294 w, 1288 w, 1285 m }	1288 w	1282	ν_{18}(E), CH$_3$ sym def (100%)
981 s		977	ν_{19}(E), CH$_3$ rock (73%), PC$_3$ antisym str (10%)
963 m, 952 m, 947 m }	952, 942 } w	944	ν_5(A$_1$), CH$_3$ rock (75%), PC$_3$ str (5%), PC$_3$ sym def (6%), SPC$_3$ str (5%)
864 m	864 w	880	ν_{20}(E), CH$_3$ rock (90%)
748 m	747, 742 } w	743	ν_{21}(E), PC$_3$ antisym str (80%), CH$_3$ rock (13%)
714 s	708 w	714	ν_6(A$_1$), PC$_3$ sym str (58%), SPC$_3$ str (25%), CH$_3$ def (7%), CH$_3$ rock (7%)
563 m	562 s[b]	564	ν_7(A$_1$), SPC$_3$ str (57%), PC$_3$ sym str (36%)
	296 m, 290 w }	292	ν_{22}(E), PC$_3$ antisym def (78%), CH$_3$ rock (16%)
282 m	278 w	286	ν_8(A$_1$), PC$_3$ sym def (m4%), CH$_3$ sym def (14%)
230 m	222 w	222	ν_{23}(E), SPC$_3$ rock (93%)

[a] Abbreviations used: m, medium; s, strong; w, weak; v, very; sh, shoulder. [b] In $(CH_3)_3P^{34}S$ the P=S stretch appears at 556 cm^{-1}; other than this there is no significant difference between the Raman spectra of $(CH_3)_3P^{32}S$ and $(CH_3)_3P^{34}S$.

Table V. Assignment of Fundamental Vibrations[a] of Trimethylphosphine-d_9 Sulfide

IR ν, cm^{-1}	Raman Δν, cm^{-1}	calc ν, cm^{-1}	assgnt and pot. energy distribn
2240 w	2237 m	2230	ν_{13}(E), CD$_3$ antisym str (96%)
2234 w	2232 s	2228	ν_1(A$_1$), CD$_3$ antisym str (100%)
2228 w		2223	ν_{14}(E), CD$_3$ antisym str (96%)
2126 w	2127 s	2079	ν_2(A$_1$), CD$_3$ sym str (100%)
	2123 sh	2078	ν_{15}(E), CD$_3$ sym str (100%)
1030 sh	1035 w	1035	ν_3(A$_1$), CD$_3$ antisym def (80%), CD$_3$ sym def (15%)
1020 m	1028 w	1032	ν_{16}(E), CD$_3$ antisym def (96%)
	1028 w	1024	ν_{17}(E), CD$_3$ antisym def (97%)
		991	ν_4(A$_1$), CD$_3$ sym def (75%), CD$_3$ antisym def (15%)
968 w		964	ν_{18}(E), CD$_3$ sym def (86%), PC$_3$ antisym str (14%)
822 s		822	ν_{21}(E), CD$_3$ rock (36%), PC$_3$ antisym str (43%), PC$_3$ antisym def (7%)
798 m	795 w, 786 w }	799	ν_6(A$_1$), CD$_3$ rock (27%), PC$_3$ sym str (28%), SPC$_3$ str (21%), CD$_3$ sym def (13%)
700 w	702 w, 698 w }	679	ν_{19}(E), PC$_3$ antisym str (31%), CD$_3$ rock (64%)
648 s	647 w	640	ν_5(A$_1$), PC$_3$ sym str (40%), CD$_3$ rock (45%), SPC$_3$ str (13%)
630 w	635 w, 630 w }	638	ν_{20}(E), CD$_3$ rock (71%), PC$_3$ antisym str (23%)
531 m	536 s	529	ν_7(A$_1$), SPC$_3$ str (56%), PC$_3$ str (37%)
	256 m	251	ν_{22}(E), PC$_3$ antisym def (75%), CD$_3$ rock (17%)
248 m	245 w	251	ν_8(A$_1$), PC$_3$ sym def (72%), CD$_3$ def (15%), CD$_3$ rock (7%)
204 m, 201 w	205 w, 198 w }	207	ν_{23}(E), SPC$_3$ rock (95%)

[a] For abbreviations see Table IV.

been aware of this potential coupling of these modes, but only with the normal-coordinate calculations could the extent of the coupling be determined.

Earlier assignments[4] for the PC$_3$ antisymmetric deformation and SPC$_3$ rocking mode are somewhat questionable. Rojhantalab et al.[4] assigned the bands at 296 cm^{-1} (256 cm^{-1} in d_9 species) and 222 cm^{-1} (205 cm^{-1} in d_9 species) to the SPC$_3$ rock and PC$_3$ antisymmetric deformation, respectively. This assignment gives an isotopic shift factor of 1.16 for the rocking motion, which is appreciably larger than that of the PC$_3$ bending motion (1.08).

We, however, have chosen to assign the 296-cm^{-1} band to the PC$_3$ antisymmetric deformation, the band at 278 cm^{-1} to the PC$_3$ symmetric deformation, and the band at 222 cm^{-1} to the SPC$_3$ rock for $(CH_3)_3PS$, as this choice places the isotopic shift factors in the order one might expect for these modes. To pursue this point further, we recorded the Raman spectrum of solid $(CH_3)_3P^{34}S$ at 24 K. The Raman band observed at 296 cm^{-1} in $(CH_3)_3P^{32}S$ appears unchanged in frequency in the ^{34}S adduct although a downward shift is anticipated if this band is assigned to the SPC$_3$ rocking motion. However, the band at 222 cm^{-1} did not appear to shift significantly either.

The assignment was checked for consistency with the Teller-Redlich product rule. For the A$_1$ modes the calculated product

Table VI. Assignment of Fundamental Vibrations[a] for Trimethylphosphine-d_3 Sulfide

IR ν, cm⁻¹	Raman Δν, cm⁻¹	calc ν, cm⁻¹	assgnt and pot. energy distribn
	2983 m	2982	ν_1(A'), CH₃ antisym str (100%)
	2983 m	2980	ν_2(A'), CH₃ antisym str (100%)
2976 w	2975 s	2979	ν_{21}(A''), ν_{22}(A''), CH₃ antisym str (100% each)
2912 w	2904 s	2895	ν_3(A'), ν_{23}(A''), CH₃ sym str (100% each)
2234 w	2237 m	2227	ν_{24}(A''), CD₃ antisym str (100%)
2228 w	2232 m	2225	ν_4(A'), CD₃ antisym str (100%)
2126 vw	2126 m	2079	ν_5(A'), CD₃ sym str (100%)
	1429 w	1426	ν_6(A'), ν_{25}(A''), CH₃ antisym def (95% each)
1420 w	1419 w	1421	ν_7(A'), CH₃ antisym def (94%)
		1421	ν_{26}(A''), CH₃ antisym def (95%)
1308 w⎫ 1300 w⎭	1302 w	1304	ν_8(A'), CH₃ sym def (100%)
1288 w	1291 w	1282	ν_{27}(A''), CH₃ sym def (100%)
1032 sh	1035 w	1030	ν_9(A'), CD₃ antisym def (94%)
1028 m	1027 w	1027	ν_{28}(A''), CD₃ antisym def (96%)
		988	ν_{10}(A'), CD₃ sym def (51%), CH₃ rock (28%), PC₃ str (12%)
964 s	950 w	961	ν_{11}(A'), CD₃ sym def (38%), CH₃ rock (50%)
944 s	933 w	928	ν_{29}(A''), CH₃ rock (68%), PC₃ antisym str (15%), CD₃ rock (6%)
	915 w	922	ν_{12}(A'), CH₃ rock (65%), CD₃ sym def (12%)
	879 vw	875	ν_{30}(A''), CH₃ rock (92%)
760 s	756 w	762	ν_{13}(A'), PC₃ sym str (57%), CD₃ rock (14%), SPC₃ str (9%), CH₃ rock (6%)
760 s		767	ν_{31}(A''), PC₃ antisym str (57%), CH₃ rock (25%), CD₃ rock (11%)
725 w	719 vw	712	ν_{14}(A'), PC₃ antisym str (60%), SPC₃ str (20%), CH₃ rock (9%)
685 s	684 w	673	ν_{32}(A''), CD₃ rock (64%), PC₃ antisym str (27%)
	657 w	651	ν_{15}(A'), CD₃ rock (62%), PC₃ sym str (31%)
552 m	553 s⎫ 544 w⎭	549	ν_{16}(A'), SPC₃ str (56%), PC₃ str (34%), CD₃ rock (6%)
	287 m	289	ν_{17}(A'), PC₃ antisym def (75%), CH₃ rock (11%), CD₃ rock (7%)
	270 w	267	ν_{33}(A''), PC₃ antisym def (76%), CD₃ rock (12%), CH₃ rock (7%)
	265 sh	274	ν_{18}(A'), PC₃ sym def (68%), CH₃ sym def (10%)
	216 w	222	ν_{34}(A''), SPC₃ rock (93%)
	208 w	211	ν_{19}(A'), SPC₃ rock (90%)

[a] For abbreviations see Table IV.

Table VII. Assignment of Fundamental Vibrations[a] for Trimethylphosphine-d_6 Sulfide

IR ν, cm⁻¹	Raman Δν, cm⁻¹	calc ν, cm⁻¹	assgnt and pot. energy distrbn
2985 w	2984 w	2979	ν_4(A'), CH₃ antisym str (100%)
2976 w	2976 m	2980	ν_{24}(A''), CH₃ antisym str (100%)
2905 w	2906 s	2895	ν_5(A'), CH₃ sym str (100%)
2233 w	2239 w	2225	ν_2(A'), CD₃ antisym str (100%)
2228 w	2234 m	2230	ν_{21}(A''), CD₃ antisym str (100%)
2228 w	2234 m	2226	ν_1(A'), CD₃ antisym str (100%)
2228 w	2234 m	2223	ν_{22}(A''), CD₃ antisym str (100%)
2122 w	2127 m	2079	ν_3(A'), CD₃ sym str (100%)
2122 w	2127 m	2078	ν_{23}(A''), CD₃ sym str (100%)
1420 w	1420 w	1425	ν_9(A'), CH₃ antisym def (95%), CH₃ rock (5%)
1412 w	1410 w	1422	ν_{28}(A''), CH₃ antisym def (95%), CH₃ rock (5%)
1294 w		1294	ν_{10}(A'), CH₃ sym def (100%)
	1037 w	1032	ν_6(A'), CD₃ antisym def (92%)
	1030 w	1031	ν_{25}(A''), CD₃ antisym def (95%)
	1030 w	1026	ν_7(A'), CD₃ antisym def (95%)
1022 s		1024	ν_{26}(A''), CD₃ antisym def (97%)
		985	ν_8(A'), CD₃ sym def (82%), CD₃ antisym def (5%), PC₃ sym str (6%)
		973	ν_{27}(A''), CD₃ sym def (64%), PC₃ antisym str (17%), CH₃ rock (15%)
922 s		933	ν_{32}(A''), CH₃ rock (54%), CD₃ def (37%)
910 sh	910 vw	915	ν_{15}(A'), CH₃ rock (68%), PC₃ sym str (10%), CD₃ def (5%)
809 m	810 w	825	ν_{14}(A'), PC₃ antisym str (45%), CD₃ rock (29%), PC₃ def (5%)
768 s	760 vw	753	ν_{13}(A'), PC₃ sym str (26%), CD₃ rock (26%), SPC₃ str (20%), CH₃ rock (13%), PC₃ def (5%)
768 s	760 vw	754	ν_{31}(A''), PC₃ antisym str (62%), CH₃ rock (14%), CD₃ rock (17%)
683 w	678 w	681	ν_{11}(A'), CD₃ rock (42%), PC₃ sym str (17%), PC₃ antisym str (34%)
	678	655	ν_{29}(A''), CD₃ rock (88%)
658 m	657 w	647	ν_{12}(A'), CD₃ rock (51%), PC₃ sym str (21%), PC₃ antisym str (16%)
	621 w	638	ν_{30}(A''), CD₃ rock (70%), PC₃ antisym str (23%)
540 m	545 s	538	ν_{16}(A'), SPC₃ str (56%), PC₃ sym str (28%), PC₃ antisym str (8%), CD₃ rock (6%)
	276 m	275	ν_{33}(A''), PC₃ antisym def (78%), CD₃ rock (14%), CH₃ rock (7%)
	256	266	ν_{18}(A'), PC₃ sym def (62%), PC₃ antisym def (9%), CD₃ def (8%), CD₃ rock (7%)
	252	252	ν_{17}(A'), PC₃ antisym def (67%), PC₃ sym def (7%), CD₃ rock (15%)
	212	215	ν_{19}(A'), SPC₃ rock (89%)
	202	207	ν_{34}(A''), SPC₃ rock (93%)

[a] For abbreviations see Table IV.

rule value is 5.42 whereas the experimental value is 5.40. Similarly, for the E modes the theoretical value is 14.2 whereas the experimental value is 13.9. These results provide support for the proposed vibrational assignment.

(CH₃)₂(CD₃)PS and (CH₃)(CD₃)₂PS. Under C_s symmetry both (CH₃)₂(CD₃)PS and (CH₃)(CD₃)₂PS will have 20 A' and 16 A'' fundamental modes of vibrations and all A' and A'' modes will be Raman as well as infrared active. With the exceptions of the CH₃/CD₃ torsional modes, all other intermolecular vibrations could be identified either in the Raman effect or in the infrared spectrum of each compound. The band assignments (Tables VI and VII), which are based on the force field for the d_0 and d_9 species, are also consistent with the results of Teller–Redlich product rule calculations where

$$\tau_{exp}(A') = 2.64; \quad \tau_{theo}(A') = 2.65$$

$$\tau_{exp}(A'') = 5.26; \quad \tau_{theo}(A'') = 5.29$$

Fermi Resonance. It will be observed that, in all three deuteriated forms of (CH₃)₃PS, the symmetric CD₃ stretching modes appear approximately at the same frequency (2127 cm⁻¹) and the observed frequency is invariably higher than the calculated values by 45–48 cm⁻¹. This difference is explained by resonance interaction between the CD₃ stretch and the first overtone of an energetically compatible CD₃ deformational mode of the same symmetry species as the CD₃ stretch. In the d_9 species the estimated frequencies of the first overtones of two CD₃ deformations,

ν_3(A₁) and ν_{16}(E) (Table V), are 2070 and 2056 cm⁻¹, respectively, and these figures are close to the calculated frequencies, 2079 and 2078 cm⁻¹, for the two CD₃ stretching fundamentals, ν_2(A₁) and ν_{15}(E), respectively. Further evidence of Fermi resonance is provided by the sharp band observed at 2013 cm⁻¹ in the Raman spectrum of (CD₃)₃PS. We assign this band to the first overtone of ν_3(A₁) or ν_{16}(E). Analogous bands appear at 2020 and 2019 cm⁻¹, respectively, in the Raman spectra of the d_6 and d_3 species.

Normal-Coordinate Calculation. Wilson's FG matrix method[6] and programs written by Schachtschneider[7] were used for the calculation of the normal coordinates for the fundamental vibrations of (CH₃)₃PS and the deuteriated species. The structural parameters used for generating the G matrices were those obtained from the analysis of the microwave spectra of these compounds. Forty internal coordinates, which were used to construct 40 symmetry coordinates, including redundancies, formed the basis set. These coordinates are analogous to those reported for the

(6) Wilson, E. B.; Decius, J. C.; Cross, P. C. *Molecular Vibrations. The Theory of Infrared and Raman Spectra*; McGraw-Hill: New York, 1955.

(7) Schachtschneider, J. H. "Vibrational Analysis of Polyatomic Molecules, V and VI"; Technical *Reports* 231-64 and 57-65, Shell Development Co.: Houston, TX, 1964, 1965.

Table VIII. Internal Force Constants for $(CH_3)_3PS$

force const	descripn	value,[a] mdyn/Å
K_q	C—H str	4.75
K_Q	P—C str	3.38
K_R	P=S str	3.78
H_α	∠HCH bend	0.52
H_β	∠HCP bend	0.55
H_ϵ	∠CPC bend	1.22
H_γ	∠SPC bend	0.66
F_q	C—H str/C—H str	0.05
F_Q	P—C str/P—C str	0.05
F_{QR}	P—C str/P=S str	0.05
$F_{q\beta}$	C—H str/∠HCP bend	−0.09
$F_{Q\beta}$	P—C str/∠HCP bend	0.40
$F_{Q\epsilon}$	P—C str/∠CPC bend	0.13
$F_{R\gamma}$	P=S str/∠SPC bend	0.08
F_β	∠HCP bend/∠HCP bend (adjacent angles)	0.004
F_β'	∠HCP bend/∠HCP bend (nonadjacent euatorial angles)	0.03
F_β''	∠HCP bend/∠HCP bend (nonadjacent axial angles)	−0.007
$F_{\epsilon\beta}$	∠CPC bend/∠HCP bend (trans)	−0.25
$F_{\epsilon\beta}'$	∠CPC bend/∠HCP bend (trans gauche)	−0.02
$F_{\epsilon\beta}'$	∠CPC bend/∠HCP bend (cis gauche)	−0.15
$F_{\beta\gamma}$	∠HCP bend/∠SPC bend	0.06

[a] All bending coordinates weighted by 1 Å.

borane and gallane adducts of trimethylphosphine, which we have previously studied.[8,9]

The initial values of the force constants of the stretching and bending modes for $(CH_3)_3P$ were chosen from previous studies,[9-13] and suitable assumptions were made for the force constants for the P=S stretch and ∠SPC bending motion. The initial force field consisted of seven diagonal force constants. To these were progressively added 14 interaction constants to obtain the best fit with the observed frequencies for the d_0 and the d_9 species. In the least-squares refinement the observed frequencies were weighted by $1/\lambda$, the Jacobian matrix being continuously checked to guide the refinement process. The 21 force constants were all retained in the final force field, and the modified values of the force constants are listed in Table VIII.

The force field constructed for $(CH_3)_3PS$ and $(CD_3)_3PS$ was used to predict the frequencies for the fundamental modes of vibrations for the partially deuteriated species, $(CH_3)_2(CD_3)PS$ and $(CH_3)(CD_3)_2PS$. Reasonably good agreement was obtained between the observed and calculated values. The average deviations of the calculated frequencies from their observed values for the d_0, d_3, d_6, and d_9 species are 0.56%, 0.83%, 0.91%, an 1.1%, respectively.

Lattice Modes. From the X-ray diffraction studies[5] of solid $(CH_3)_3PS$, it was shown that the crystal has a monoclinic structure (C_{2h}^2) with two molecules per unit cell, each lying on a C_s plane. From this factor group one predicts nine spectroscopically active lattice modes with the following representations and activities:

$$\Gamma(OT) = 2A_g(R) + 1B_g(R)$$

$$\Gamma(OL) = 1A_g(R) + 2B_g(R) + 1B_u(IR) + 2A_u(IR)$$

In the Raman spectrum of a single crystal of $(CH_3)_3PS$ measured at liquid nitrogen temperature, Rojhantalab et al.[4] observed five of the nine possible Raman-active lattice modes, all of which appeared below 110 cm^{-1}. In the corresponding spectrum of $(CD_3)_3PS$ only four bands were observed in the same spectral

region. However, no definitive assignment of any of the observed lattice frequencies was made by these investigators. In the room-temperature studies of the Raman spectra of the polycrystalline forms of $(CH_3)_3PS$ and $(CD_3)_3PS$, we observed three weak bands in both cases, which are attributable to lattice vibrations. These bands appear at 90, 65, and 57 cm^{-1} for the light compound and shift to 85, 61, and 55 cm^{-1} in the spectrum of the deuteriated species. The frequency shifts for the first two analogous bands of the light and deuteriated compounds are 1.06 and 1.07, respectively, and these values are in agreement with the calculated values of the isotopic shift factors of 1.08 for librations around the B or C molecular axis. The smaller ratio of 1.04, observed for the third band, is consistent with an intermolecular translational motion for which the calculated value of the isotopic shift factor is equal to 1.04.

In the far-infrared spectrum of $(CH_3)_3PS$, recorded at room temperature, we observed three distinct bands at frequencies of 98, 75, and 55 cm^{-1}. The corresponding bands in the d_9 species are observed at 91, 71, and 53 cm^{-1}, although the latter compound shows additional bands in this spectral region. We assign the three observed bands in the light compound and the analogous bands in the deuteriated species to the three possible librational motions $(2A_u + 1B_u)$. For the first two bands the observed ratios of 1.06 and 1.08 are in good agreement with the calculated value of 1.08. However, for the third infrared band a rather large difference is found between the observed isotopic shift factor of 1.04 and those calculated for the librational modes. In fact, the shift factor for the librational mode around the A axis should be ∼1.13 and it may be because of anharmonicity that it is significantly less. Nevertheless, if the space groups is correct, then the three infrared bands ought to be arising from the three librational motions.

Discussion

The P–S and P–C bond distances as well as the SPC bond angle in $(CH_3)_3PS$, obtained from an analysis of the microwave spectra of five isotopic species, are in good agreement with those reported earlier from electron diffraction studies.[1] Of special importance is the short phosphorus–sulfur bond length (1.936 Å), which indicates that the bond order for this bond is much larger than that of a single bond. The higher bond order for this bond is best explained by a bond type having a σ and a π component that transfer the electronic charges in opposite directions.

At first sight, structure I for $(CH_3)_3P=S$ appears more acceptable, as in this structure all the HCH angles are equal (109.41 ± 0.04°) and all the HCP angles are also equal (109.53 ± 0.04°), whereas a large difference between ∠PCH^s (113.17 ± 1.25°) and ∠PCH^a (107.52 ± 0.04°) is observed in structure II. However, the C–H bond length in structure II (1.094 ± 0.03 Å) is preferred to the rather short C–H bond (1.087 ± 0.002 Å) proposed in structure I. It is reasonable to assume the existence of a methyl group tilt toward the phosphorus–sulfur double bond, since evidence of tilted methyl groups has been presented in a number of cases where CH$_3$ is bonded either to an unsaturated atom or to an atom that has an unshared electron pair.[14,15] A recent redetermination by the present investigators of the molecular structure of trimethylphospine[16] from the microwave spectra of seven isotopic species shows that the methyl groups retain their symmetry axis and are tilted toward the unshared electron pair of the P atom by approximately 1.7 ± 0.2°. It should be noted that, in order to discern subtle structure variations from the listed parameters, it would be necessary to examine the microwave spectra of the d_1^s and d_1^a isotopic species as well as possibly a ^{13}C isotopic species. Certainly, these data would give more information on the structural parameters for the methyl groups. However, minor differences in these parameters would not be expected to

(8) Odom, J. D.; Hudgens, B. A.; Durig, J. R. *J. Phys. Chem.* **1973**, *77*, 1972.
(9) Odom, J. D.; Chatterjee, K. K.; Durig, J. R. *J. Phys. Chem.* **1980**, *84*, 1843.
(10) Odom, J. D.; Chatterjee, K. K.; Durig, J. R. *J. Mol. Struct.* **1981**, *74*, 193.
(11) Durig, J. R.; Bradley, C. B.; Odom, J. D. *Inorg. Chem.* **1982**, *21*, 1466.
(12) Durig, J. R.; Chatterjee, K. K. *J. Mol. Struct.* **1982**, *81*, 167.
(13) Drake, J. E.; Hencher, J. L.; Rapp, B. *Inorg. Chem.* **1977**, *16*, 2289.

(14) Wollrab, J. E. *Rotational Spectra and Molecular Structure*; Academic Press: New York, 1967.
(15) Durig, J. R.; Chatterjee, K. K.; Lindsay, N. E.; Groner, P. *J. Am. Chem. Soc.* **1986**, *108*, 6903.
(16) Durig, J. R.; Chatterjee, K. K.; Bell, Stephen. To be submitted for publication.

significantly alter the structural parameters for the heavy atoms.

In the electron diffraction investigation of the structure of trimethylphosphine sulfide, two different models were utilized, i.e., partially rotated methyl groups and methyl groups freely rotating. The model with the methyl groups rotated by 42.7 ± 7.3° appeared to give a better fit to the diffraction pattern. The substitution of all three hydrogens on one of the methyl groups by deuterium does not provide data for checking the partially rotated model. A model with tilted methyl groups was not tried in the electron diffraction investigation, but is is expected that it would provide as good a fit to the diffraction curves as the partially rotated model. There have been many cases where "tilted" methyl groups have been found[14] but little evidence for partially rotated methyl groups.

Results obtained from measurements of the infrared spectra of solid $(CH_3)_3PS$ and $(CD_3)_3PS$ at low temperature contradict some of the assignments made by Rojhantalab et al.[4] from the study of the Raman spectra alone. Changes have been presented for the assignments of the CH_3 rocks, the PC_3 skeletal modes, and possibly the SPC_3 rocking modes. For $(CH_3)_3PS$ and the isotopic species, the fundamental frequencies of the carbon–hydrogen stretching and bending motions fall within the same range as those observed[16-19] for the corresponding modes in $(CH_3)_3P$. This indicates that the force constants for methyl stretching and bending motions are not affected by bonding to the sulfur atom. On the other hand, the frequencies for the PC_3 skeletal motions are significantly altered. The force constant for the PC_3 stretch increases from 2.78 mdyn/Å in the free base to 3.38 mdyn/Å in the sulfur adduct. This increase in the magnitude of the PC_3 stretching force constant is consistent with the shortening of the

P–C bond length from 1.846 Å in $(CH_3)_3P$[16] to 1.814 Å in $(CH_3)_3PS$. The CPC bond angle increases from 98.9° in the free base[16] to 104.41° in the sulfur adduct. In all previous studies on the adducts of trimethylphosphine,[8-10,12] similar changes in the geometry of $(CH_3)_3P$ upon adduct formation has been accompanied by an increase in the magnitude of the PC_3 stretching force constant. These observations have been explained by the VSEPR model.

The potential energy distributions (Tables V–VII) for the observed bands show an abundance of mixing among the fundamental modes of vibrations. For instance, the P=S and PC_3 stretching motions couple extensively and a very large degree of mode mixing is also observed between the CD_3 rocking and PC_3 stretching motions. Each of the five interaction constants, F_β', F_β'', $F_{\epsilon\beta}$, $F_{\epsilon\beta}'$ and $F_{\epsilon\beta}''$ (table VIII), affect the relative energies of the methyl rocking motions. While the mechanisms behind the interactions are not obvious in all cases, the interaction F_β' may be interpreted as a measure of the repulsive force between the equatorial hydrogen atoms of the three different methyl groups of the molecule.

The fact that the three observed infrared bands in the spectral range for lattice modes have shift factors and frequencies very similar to those of Raman lines observed in the spectrum of the corresponding molecule suggests that the Raman lines are probably due to librational modes. There is also evidence that the infrared bands may be doublets, which would indicate that the tentative determined space groups is not correct. Far-infrared spectral studies of an oriented single crystal would provide additional information on the crystal symmetry.

(17) McKean, D. C.; McQuillan, G. P. *Spectrochim. Acta* **1983**, *39A*, 293.
(18) Rosenbaum, E. J.; Rubin, D. R.; Sandberg, C. R. *J. Chem. Phys.* **1940**, *8*, 366.
(19) Park, P. J. D.; Hendra, P. J. *Spectrochim. Acta* **1968**, *24A*, 2081.

Contribution from the Laboratoire de Chimie Quantique, ER 139 DU CNRS, Université Louis Pasteur, 4, rue Blaise Pascal, F 67000 Strasbourg, France

CO_2 Interaction with $HCr(CO)_5^-$: Theoretical Study of the Thermodynamic Aspects

C. Bo and A. Dedieu*

Ab initio LCAO-MO-SCF calculations have been carried out for the acid–base adduct involved in the insertion reaction of CO_2 into the metal–hydrogen bond of $HCr(CO)_5^-$. This adduct, the geometry of which has been determined, is found to be more stable than the reactants. Its further evolution toward the formate product and the role of an ancillary ligand dissociation are discussed in terms of molecular orbital interactions.

There is much current interest in carbon dioxide coordination and reactivity. The insertion reaction of CO_2 into the metal-hydride bond of hydrido transition-metal complexes (reaction 1)

$$CO_2 + L_nMH \rightarrow L_nM(OCHO) \qquad (1)$$
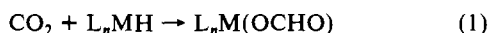
is observed in several instances[1,2] and has been one of the most thoroughly investigated reactions, especially from the point of view

of its mechanism, owing to its apparent simplicity and its prototype character. Experimental studies using the $HM(CO)_5^-$ hydrido carbonyl complexes (M = Cr, Mo, W) as substrates[3-6] have shown that, at variance with the insertion into a metal–alkyl bond,[7,8] the insertion into the metal–hydride bond probably involves the dissociation of an ancillary carbonyl ligand. This dissociation might be triggered by a preassociation of the hydrido complex with CO_2.[4] Support for this hypothesis was gained from the

(1) For reviews, see for instance: (a) Darensbourg, D. J.; Kudaroski, R. A. *Adv. Organomet. Chem.* **1983**, *22*, 129. (b) Palmer, D. A.; Van Eldik, R. *Chem. Rev.* **1983**, *83*, 51. (c) Ziessel, R. *Nouv. J. Chim.* **1983**, *7*, 613. (d) Darensbourg, D. J.; Ovalles, C. *Chem Tech* **1985**, *15*, 636. (e) Walther, D. *Coord. Chem. Rev.* **1987**, *79*, 135. (f) Braunstein, P.; Matt, D.; Nobel, D. *Chem. Rev.* **1988**, *88*, 747.
(2) For more recent examples, see: (a) Fong, L. K.; Fox, J. R.; Cooper, N. J. *Organometallics* **1987**, *6*, 223. (b) Kundel, P.; Berke, H. *J. Organomet. Chem.* **1986**, *314*, C31. (c) Sullivan, B. P.; Meyer, T. J. *Organometallics* **1986**, *5*, 1500.

(3) Darensbourg, D. J.; Rokicki, A.; Darensbourg, M. Y. *J. Am. Chem. Soc.* **1981**, *103*, 3223.
(4) Darensbourg, D. J.; Rokicki, A. *Organometallics* **1982**, *1*, 1685.
(5) Darensbourg, M. Y.; Bau, R.; Marks, M. W.; Burch, R. R., Jr.; Deaton, J. C.; Slater, S. *J. Am. Chem. Soc.* **1982**, *104*, 6961.
(6) Darensbourg, D. J.; Pala, M. *J. Am. Chem. Soc.* **1985**, *107*, 5687.
(7) Darensbourg, D. J.; Kudaroski Hanckel, R.; Bauch, C. G.; Pala, M.; Simmons, D.; White, J. N. *J. Am. Chem. Soc.* **1985**, *107*, 7463.
(8) Darensbourg, D. J.; Grotsch, G. *J. Am. Chem. Soc.* **1985**, *107*, 7473.